HHS Public Access

Author manuscript

J Child Neurol. Author manuscript; available in PMC 2016 June 01.

Published in final edited form as:

J Child Neurol. 2015 June ; 30(7): 842–849. doi:10.1177/0883073814544364.

Rates and characteristics of radiographically detected intracerebral cavernous malformations after cranial radiation therapy in pediatric cancer patients

Erica Gastelum, MD[#1], **Katherine Sear, MPH**[#2], **Nancy Hills, PhD**[2,3], **Erika Roddy, BA**[2], **Dominica Randazzo, BS**[2], **Nassim Chettout, MD**[2], **Christopher Hess, MD PhD**[4], **Jennifer Cotter, MD**[5], **Daphne A. Haas-Kogan, MD**[6,7], **Heather Fullerton, MD MAS**[2,6], and **Sabine Mueller, MD PhD**[2,6,8]

[1]Department of Pediatrics, University of California, San Francisco – Fresno

[2]Department of Neurology, University of California, San Francisco

[3]Epidemiology& Biostatistics, University of California, San Francisco

[4]Radiology, University of California, San Francisco

[5]Pathology, University of California, San Francisco

[6]Pediatrics, University of California, San Francisco

[7]Radiation Oncology, University of California, San Francisco

[8]Neurosurgery, University of California, San Francisco

[#] These authors contributed equally to this work.

Abstract

Rates and characteristics of intracerebral cavernous malformations (ICMs) after cranial radiation therapy (CRT) remain poorly understood. Herein we report on ICMs detected on follow+up imaging in pediatric cancer patients who received CRT at age ≤ 18 years from 1980 to 2009. Through chart reviews (n=362) and phone interviews (n=104) of a retrospective cohort we identified 10 patients with ICMs. The median latency time for detection of ICMs after CRT was 12 years (range 1+24 years) at a median age of 21.4 years (IQR 15+28). The cumulative incidence was 3% (95% CI 1+8%) at 10 years post CRT and 14% (95% CI 7+26%) at 15 years. Three patients underwent surgical resection. Two surgical specimens were pathologically similar to

Corresponding Author: Sabine Mueller MD PhD Department of Neurology, Neurosurgery and Pediatrics University of California, San Francisco Sandler Neuroscience Building 675 Nelson Rising Lane, Room 402C San Francisco, CA 94148 Phone: 415+502+7301 | Fax: 415+502+7299 muellers@neuropeds.ucsf.edu.

Author Contributions

EG, KS, HF and SM conceived and designed the study and also drafted the manuscript. EG, KS, ER, DR, NC, CH, JC, DHK, SM acquired the data. EG, KS, NH, JC, CH, HF and SM analyzed and interpreted the data. EG, KS, NH, ER, CH, JC, DHK, HF and SM critically revised the manuscript for important intellectual content. SM and HF supervised the study. All authors read and approved the final manuscript.

Declaration of Conflicting Interests

The authors declared no potential conflicts of interest with respect to the research, authorship, and/or publication of this article.

Ethical Approval

This study was approved by the Institutional Review Board (# 10+01049) of the University of California, San Francisco.

sporadically occurring ICMs; one was consistent with capillary telangiectasia. ICMs are common after CRT and can show a spectrum of histological features.

Keywords

intracerebral cavernous malformation; cranial radiation therapy; pediatric cancer survivors

Introduction

Intracerebral cavernous malformations (ICMs) are increasingly recognized as one of the long+term sequelae of cranial radiation therapy (CRT), especially in pediatric populations [1-5]. While the majority of these ICMs are asymptomatic, symptomatic lesions can present with seizure, new headache, and focal neurologic deficits due to hemorrhagic stroke. Pathologically, ICMs are characterized by a circumscribed cluster of dilated vascular sinusoids lined by a single endothelial layer, with little to no intervening brain parenchyma [1-5]. Intralesional or perilesional deposits, including thrombus, calcification, and cysts are common, and ICMs are often bordered by hemosiderin and reactive gliosis. On MRI, ICMs present as mixed signal lesions of low and high intensity surrounded by a complete rim of T1 hypointensity. This “popcorn” appearance corresponds to the mixture of blood products at various stages of degradation within and around the lesion.

The prevalence of ICMs has been reported to be 0.4+0.6% in the general population; however, the incidence of ICMs after CRT remains largely unknown [6-9]. A few studies have reported that ICMs occur within the field of prior radiation as early as five months, with the majority occurring 3+10 years after CRT [1, 4]. The precise relationship between CRT dose and ICM development, however, is still unclear. Some studies have found a dose+dependent relationship noting decreased latency to ICM development in those who receive higher radiation doses [1, 5, 10]. Others report an inverse relationship, finding that ICMs occur more commonly at the lower dose rim of the radiation field [5, 11]. Regardless, it appears that low +dose radiation is sufficient to induce ICMs, as children with leukemia, who are treated with relatively low doses of radiation (12+24 Gy), are also at increased risk for developing ICMs [11, 12].

There are conflicting reports as to whether radiation+induced ICMs differ pathologically from congenital/spontaneously occurring ICMs [1, 13-16]. Clinically, radiation+ induced ICMs also appear to carry an increased risk of hemorrhage, reported at 3.9% per patient+year as compared to 0.25% in spontaneous ICMs [5, 7].

In this study, we assessed the incidence of radiographically detected ICMs in a single+center retrospective cohort of patients who received CRT during childhood. When available we reviewed pathology in order to further characterize the histologic features of radiation +induced ICMs.

Materials and Methods

We performed a retrospective cohort study of patients identified through the University of California, San Francisco (UCSF) Cancer Registry who received treatment at UCSF with CRT at age ≤ 18 years between 1980 and 2009. This cohort was previously described [17].

We identified 385 eligible patients whom we contacted through mail and invited to participate in the study. Twenty+three patients declined and were excluded from the study. Chart review was conducted for the remaining 362 patients, and of those, 104 (or surrogates when necessary) consented/assented to telephone interviews. Interviews were carried out with either the patient (if alive and ≥ 18 years of age at the time of the study; n=71), or the legal guardian of the patients currently < 18 years of age (n=20), or deceased (n=13). Information gathered during chart review and/or interview included baseline demographics (age, sex, race), primary cancer diagnosis and cancer treatment, age and date of diagnosis, radiation dose and treatment time, date of initial MRI to detect primary cancer diagnosis, and date of last MRI follow+up at our institution. Primary cancer diagnosis was based on pathology report, and date of surgery was confirmed by operative report. ICM identified by chart review was defined as physician documentation of ICM and/or brain imaging report that indicated ICM. Nine ICM patients were identified by chart review. ICM identified by interview was defined as participant report of a healthcare provider communicating the diagnosis to the patient. One ICM patient was identified on interview, and the patient's diagnosis was subsequently confirmed by chart and imaging review. For all patients with a diagnosis of ICM, all relevant brain imaging was obtained and reviewed by a study neuroradiologist (CH), who confirmed presence or absence of ICM, and specified anatomic locations for each ICM. For patients with ICM, additional information gathered by chart review included interval timing of imaging follow+up after CRT, and ICM related symptoms or treatment. Pathology specimens were obtained and reviewed in detail by a trained pathologist (JC) for all patients who underwent resection of the ICM. Data from medical records and imaging for all patients, including those who did not have ICMs, were collected through September 2011.

Statistical Analysis

Survival analysis was used to determine cumulative incidence of radiographically defined ICM after CRT. The primary outcome was time to radiographic appearance of ICM, calculated from last day of CRT to the date of first MRI with evidence of ICM. Censoring criteria were death, evidence of ICM or last follow+up MRI without evidence of ICM. For all patients with evidence of ICM, we confirmed that initial diagnostic imaging and follow +up MRI after completion of CRT was negative for ICM until date of diagnosis. Most patients were followed with MRI scans at regular time intervals, every 1 to 2 years. To calculate incidence rates we used the midpoint of the interval between CRT/last normal MRI and first detection. For two patients who did not receive regular MRI follow+up, the median time between end of CRT and date of initial radiographic evidence of ICM was used as an estimate for our analysis. Because our primary goal was to estimate incidence and not to determine factors associated with time to occurrence of ICM, we did not account for the fact

that our data were interval censored, given that actual time of ICM development cannot be known. Rather, we used detection date to calculate incidence rates.

Results

Patient characteristics

Of the 362 eligible patients, we excluded 123 given that these patients had no MRI after completion of radiation therapy (Figure 1, supplemental Table 1). For the 239 patients, median age at time of CRT was 8.7 years (IQR, 4.6+13.0), and median age at last follow up was 15.1 years (IQR, 9.6+19.3). The majority of the patients were alive (n=165; 69%) at time of interview and/or chart review (Table 1, 2).

Radiographically detected ICM

In our cohort of 239 participants, we identified 10 patients with a diagnosis of ICM and all were confirmed radiographically. Figures 2 and 3 show representative MRI images of confirmed ICMs, revealing well+circumscribed lesions with heterogeneous T1 and T2 signal, with surrounding hemosiderin and varying degrees of calcification and gliosis. Of the 10 identified patients with ICMs, eight had had MRI follow+up every 1+2 years from the time of their CRT to their ICM diagnosis, while two patients were lost to follow+up after their initial CRT. These two patients underwent MRI more than 10 years after completion of CRT, at which time ICM was noted on imaging.

Baseline demographics of the patients with ICMs show that most were male (n=8; 80%). Nine out of 10 patients with ICMs received CRT doses >50 Gy (range 54+ 66 Gy) and one patient received low dose CRT of 24 Gy. Seven out of the 10 ICMs were located within the brain region that received high+dose CRT whereas the remaining three were located in the periphery of the radiation field (Table 2). Median age at CRT was 9.7 years (IQR= 7.9+13.7) and median latency of ICM diagnosis (defined as time from CRT to midpoint between last cavmal+free MRI and cavmal diagnosis MRI) was 11.6 years post CRT (IQR= 4.3+12.8) (Figure 4). Median latency decreases slightly to 9.0 if the two children with long intervals between last cavmal+free MRI and diagnosis MRI are excluded, but IQRs for this latency period remain largely unchanged ((3.9+12.6). The overall rate of radiographically detected ICM was 584 per 100,000 person years (95% CI 538+633). The cumulative incidence of radiographically detected ICM was 2% (95% CI 0.6+6%) at 5 years, 3% (95% CI 1+8%) at 10 years, and 14% (95% CI 7+26%) at 15 years.

Characteristics of ICM on Pathology

Of the 10 patients with radiographically detected ICMs, three patients underwent surgical resection for symptoms attributed to these lesions. Symptoms included new onset of headache plus seizures (patient 4), worsening headache (patient 5) and left+ sided numbness, left facial droop, left visual field defect, and decreased strength on the left side (patient 10). Two patients had resection specimens that were morphologically similar to spontaneously occurring or congenital ICMs. These specimens demonstrated thin+walled dilated loops of non+arterial vessels with little to no intervening brain tissue, and adjacent hemosiderin+laden macrophages. The third specimen exhibited characteristics of a

telangiectasia, with smaller, capillary+like vascular lumina separated by intervening brain parenchyma (Figure 3).

DISCUSSION

In this single+center retrospective cohort study, we found that children undergoing CRT for cancer therapy are at high risk for developing ICMs years after their initial therapy. Symptomatic radiation+induced+ICMs that are classified as such on imaging represent a spectrum of vascular disorders on histology ranging from capillary telangiectasia to a more classic ICM appearance. The cumulative incidence of ICMs after CRT has been estimated at 3.9% and 5.0% within 10 and 15 years post CRT, respectively [3]. In our cohort of pediatric cancer patients treated with CRT, the cumulative incidence of post+CRT ICM was found to be slightly higher at 3% at 10 years and 14% at 15 years however due to our small sample number the 95% CI are relatively large and that difference might not be statistically significant. Not all patients in our cohort, however, underwent imaging most sensitive to ICM detection, such as gradient echo imaging at high field strengths. Some ICMs may therefore have remained undetected, and our results likely underestimate the true incidence in this cohort.

Our study period spanned 29 years, and most cases of ICM were documented in the last 10 years of the study, with the majority of ICMs documented in the last 5 years of the study. Although there is literature reporting radiographic identification of ICMs decades before the onset of our study period, the identified ICMs in the later years of our study could reflect the significant evolution in imaging technology, or even an increased awareness of ICM's among radiologists. Hence, these are additional factors that could have potentially contributed to underreporting of ICMs in the earlier years of the study.

Radiation+induced ICMs are known to develop over a long time period after CRT: in our cohort, 1 to 24 years after radiation. The median latency time to detection was 9 years; however, imaging was not done systematically at specific time points for all patients, so the exact latency could not be determined. Prior reports have estimated very similar latency times, ranging from 3 months to 22 years [11, 16, 18]. These results suggest that pediatric cancer patients treated with CRT who present with new neurological findings should be also assessed for ICMs as a potential underlying diagnosis.

Young age at time of CRT has been associated with an increased risk of developing ICMs [1, 2, 5]. Vinchon *et al.*, however, reported that receiving CRT at an older age was a risk factor for developing ICMs [19]. In our cohort, seven children were ≤ 12 years of age at time of CRT, while only three were treated with CRT at age >12 years. Although the rate of ICM detection per 100,000 person+years did not significantly differ between the <12 years age group (595, 95% CI 548+644, n=7) and the >12 years group (559, 95% CI 514+607, n=3), given the small sample size of the groups we cannot rule out the possibility that we lacked the power to detect a true difference.

Vascular malformations after CRT can exhibit heterogenous histopathology. A study by Baumgartner *et al.* found that radiation+induced ICMs are pathologically identical to

sporadic and familial ICMs [16]. However, as Pozzatti *et al.* note, naturally occurring ICMs usually display elements that suggest a prolonged development, including calcification [20]. In our study, two of the three pathological specimens showed classic appearance of ICMs and had no evidence of calcifications, whereas the other specimen was consistent with telangiectasia with evidence of calcifications. Although the pathogenesis of radiation +induced ICMs is not well understood, it has been proposed that they result from radiation +induced injury to the vasculature that histologically manifests as fibrinoid necrosis, hyalinization, and edema. Such changes can cause narrowing of the vascular lumen, leading to ischemia and the release of angiogenic factors, thus inducing dilation and proliferation of thin+walled vessels in adjacent areas [21]. While ICM and capillary telangiectasia are considered separate, pathologically defined entities, they can have a similar imaging appearance, and some authors have proposed that they may be part of the same disease spectrum, representing early and late phases of radiation+induced vasculopathy, respectively [22]. Although our sample size is small, our results are consistent with prior observations of pathological variation among radiographically detected ICMs.

Eight out of our 10 radiographically detected ICMs were found in male patients. This male predominance is supported by a review of the literature of radiation+induced ICMs and other small case series [4, 11]. However, others have found no gender predilection in the development of ICMs after CRT [18]. More studies with greater numbers are needed to assess whether a gender predilection is present in the risk of ICM development following CRT.

In our study, nine out of 10 patients with ICM had a CRT dose of >30 Gy, suggesting that higher CRT doses may confer an increased risk of developing ICM. Our results are supported by multiple prior studies reporting an association between CRT dose >30 Gy and increased ICM incidence [3, 4, 11]. Similarly, our cohort reflects previously published data that most CRT+associated ICMs are asymptomatic [3, 12], as only three of our 10 radiographically detected ICMs required surgical intervention for symptom control.

It has been reported that risk of hemorrhage may be significant among pediatric patients with CRT+induced ICMs [11]. However, no patients in our cohort presented with or subsequently developed a symptomatic hemorrhage during our follow up period. In one study, out of 419 patients who received CRT, 9 developed ICMs, and 3 of those developed symptomatic hemorrhagic ICMs requiring surgical intervention [11]. By contrast, the rate of symptomatic hemorrhage in sporadically occurring ICMs in the general population is only 2.4% per patient year [6]. Studies showing a higher bleeding risk for CRT+induced ICMs had small cohorts of six to nine patients with ICMs; therefore larger, prospective studies are needed to further clarify this risk.

Conclusion

Radiation induced ICMs are frequent in patients who underwent CRT and occur on a histopathological spectrum.

Supplementary Material

Refer to Web version on PubMed Central for supplementary material.

Acknowledgements

This work was presented at the Child Neurology Society 41st Annual Meeting, October 31 – November 3 2012, Huntington Beach, CA.

Funding

The work was supported by a donation from the LaRoche family (HF), the Hellman Fellow Fund (SM), and the National Center for Advancing Translational Sciences, National Institutes of Health, through UCSF+CTSI Grant Number KL2TR000143 (SM).

References

1. Larson JJ, Ball WS, Bove KE, Crone KR, Tew JM Jr. Formation of intracerebral cavernous malformations after radiation treatment for central nervous system neoplasia in children. Journal of neurosurgery. 1998; 88(1):51–6. [PubMed: 9420072]
2. Heckl S, Aschoff A, Kunze S. Cavernomas of the skull: review of the literature 1975-2000. Neurosurgical review. 2002; 25(1-2):56–62. discussion 6-7. [PubMed: 11954766]
3. Strenger V, Sovinz P, Lackner H, et al. Intracerebral cavernous hemangioma after cranial irradiation in childhood. Incidence and risk factors. Strahlentherapie und Onkologie : Organ der Deutschen Rontgengesellschaft [et al]. 2008; 184(5):276–80.
4. Nimjee SM, Powers CJ, Bulsara KR. Review of the literature on de novo formation of cavernous malformations of the central nervous system after radiation therapy. Neurosurgical focus. 2006; 21(1):e4. [PubMed: 16859257]
5. Keezer MR, Del Maestro R. Radiation-induced cavernous hemangiomas: case report and literature review. The Canadian journal of neurological sciences Le journal canadien des sciences neurologiques. 2009; 36(3):303–10. [PubMed: 19534329]
6. Gross BA, Lin N, Du R, Day AL. The natural history of intracranial cavernous malformations. Neurosurgical focus. 2011; 30(6):E24. [PubMed: 21631226]
7. Del Curling O Jr. Kelly DL Jr. Elster AD, Craven TE. An analysis of the natural history of cavernous angiomas. Journal of neurosurgery. 1991; 75(5):702–8. [PubMed: 1919691]
8. Otten P, Pizzolato GP, Rilliet B, Berney J. [131 cases of cavernous angioma (cavernomas) of the CNS, discovered by retrospective analysis of 24,535 autopsies]. Neuro-Chirurgie. 1989; 35(2):82–3. 128–31. [PubMed: 2674753]
9. Sarwar M, McCormick WF. Intracerebral venous angioma. Case report and review. Archives of neurology. 1978; 35(5):323–5. [PubMed: 646686]
10. Heckl S, Aschoff A, Kunze S. Radiation-induced cavernous hemangiomas of the brain: a late effect predominantly in children. Cancer. 2002; 94(12):3285–91. [PubMed: 12115362]
11. Duhem R, Vinchon M, Leblond P, Soto-Ares G, Dhellemmes P. Cavernous malformations after cerebral irradiation during childhood: report of nine cases. Child's nervous system : ChNS : official journal of the International Society for Pediatric Neurosurgery. 2005; 21(10):922–5.
12. Faraci M, Morana G, Bagnasco F, et al. Magnetic resonance imaging in childhood leukemia survivors treated with cranial radiotherapy: a cross sectional, single center study. Pediatric blood & cancer. 2011; 57(2):240–6. [PubMed: 21671360]
13. Alexander MJ, DeSalles AA, Tomiyasu U. Multiple radiation-induced intracranial lesions after treatment for pituitary adenoma. Case report. Journal of neurosurgery. 1998; 88(1):111–5. [PubMed: 9420081]
14. Gewirtz RJ, Steinberg GK, Crowley R, Levy RP. Pathological changes in surgically resected angiographically occult vascular malformations after radiation. Neurosurgery. 1998; 42(4):738–42. discussion 42-3. [PubMed: 9574637]
15. Maraire JN, Abdulrauf SI, Berger S, Knisely J, Awad IA. De novo development of a cavernous malformation of the spinal cord following spinal axis radiation. Case report. Journal of neurosurgery. 1999; 90(2 Suppl):234–8. [PubMed: 10199254]

16. Baumgartner JE, Ater JL, Ha CS, et al. Pathologically proven cavernous angiomas of the brain following radiation therapy for pediatric brain tumors. Pediatric neurosurgery. 2003; 39(4):201–7. [PubMed: 12944701]

17. Mueller S, Sear K, Hills NK, et al. Risk of first and recurrent stroke in childhood cancer survivors treated with cranial and cervical radiation therapy. International journal of radiation oncology, biology, physics. 2013; 86(4):643–8.

18. Burn S, Gunny R, Phipps K, Gaze M, Hayward R. Incidence of cavernoma development in children after radiotherapy for brain tumors. Journal of neurosurgery. 2007; 106(5 Suppl):379–83. [PubMed: 17566205]

19. Vinchon M, Leblond P, Caron S, Delestret I, Baroncini M, Coche B. Radiation-induced tumors in children irradiated for brain tumor: a longitudinal study. Child's nervous system : ChNS : official journal of the International Society for Pediatric Neurosurgery. 2011; 27(3):445–53.

20. Pozzati E, Giangaspero F, Marliani F, Acciarri N. Occult cerebrovascular malformations after irradiation. Neurosurgery. 1996; 39(4):677–82. discussion 82-4. [PubMed: 8880758]

21. Poussaint TY, Siffert J, Barnes PD, et al. Hemorrhagic vasculopathy after treatment of central nervous system neoplasia in childhood: diagnosis and follow-up. AJNR American journal of neuroradiology. 1995; 16(4):693–9. [PubMed: 7611024]

22. Humpl T, Bruhl K, Bohl J, Schwarz M, Stoeter P, Gutjahr P. Cerebral haemorrhage in long-term survivors of childhood acute lymphoblastic leukaemia. European journal of pediatrics. 1997; 156(5):367–70. [PubMed: 9177978]

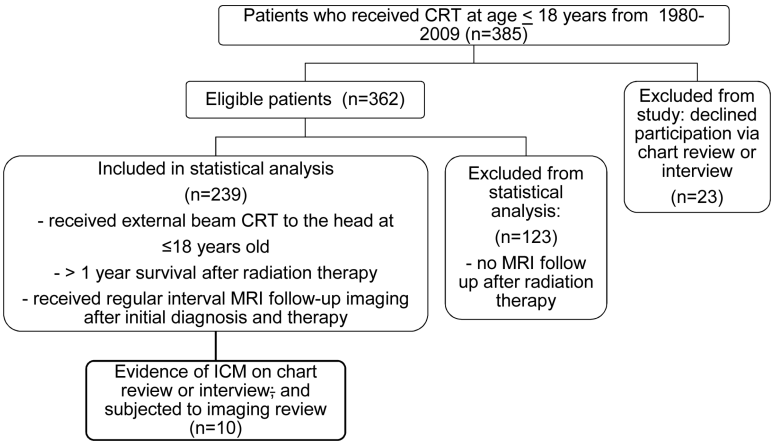

Figure 1.

Flow diagram demonstrating the recruitment and participation of the 239 patients within the final study cohort.

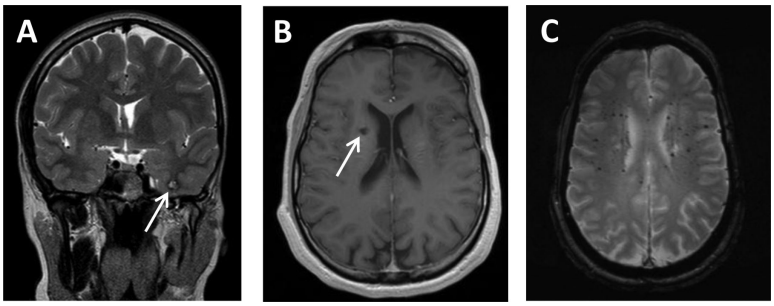

Figure 2.

MRI appearance of vascular malformations: **A:** Example of classic MRI appearance of intracranial cavernous malformation (ICM) on T2+weighted imaging (Patient 3). Inferior left temporal lobe ICM showing complete low signal rim surrounding an area of mixed T2 signal. **B,C**: Radiographic spectrum of vasculopathies in the same patient (Patient 9): **B** gadolinium+enhanced T1+weighted image showing a right periventricular ICM with small area of hyperintensity surrounded by a hypointense signal, and **C**: T2*+weighted image showing small and scattered radiation related microbleeds shown as areas of decreased signal intensity.

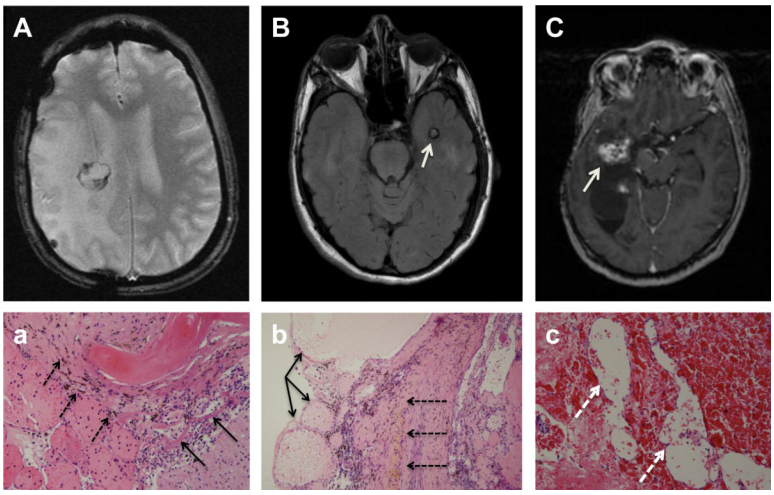

Figure 3.

MRI images of three patients who underwent surgical resection for symptomatic ICMs and the corresponding pathology. MRI images of radiographically identified ICMs are shown in A+C. **A (Patient 4):** T2*+weighted, **B (Patient 5): T2 FLAIR, C (Patient 10)**: T1+weighted MRI. **A** and **B** depict the typical appearance of ICM (white arrow) on MRI with a core of mixed increased and decreased signal intensity surrounded by low signal intensity from adjacent hemosiderin+laden parenchyma. Corresponding pathology (**a,b**) showing classic ICM with abnormal thin walled, dilated non+arterial blood vessels (black thin arrows) with little to no intervening brain tissue surrounded by a rim of hemosiderin +laden macrophages (black dashed arrows) in the adjacent parenchyma. **C** shows a right temporal+parietal ICM (white arrow) with high signal intensity and (**c**) corresponding pathology with dilated capillary+like vascular spaces (white dashed arrows) separated by intervening tissue.

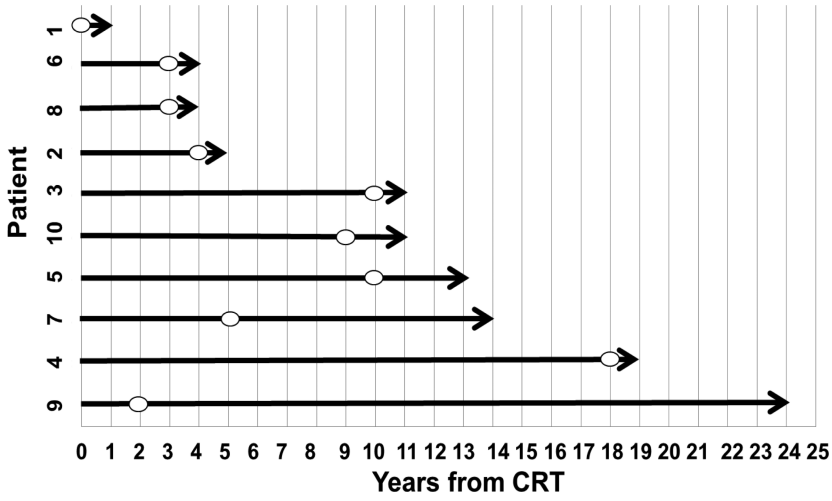

Figure 4.

Overview of time to detection of ICM on MRI per individual patient. The figure depicts the latency time from the end of CRT to the time ICM was first detected on MRI. The symbol (o) denotes each patient's last MRI follow+up free of evidence of any lesion meeting radiographic criteria of ICM. Of note, imaging was not systematically acquired at specific time points therefore latency to radiographic detection of ICM is an estimate.

Table 1

Patient characteristics of cohort

Characteristic	Patients with ICM (n=10) n (%)	Total cohort (n=229) n (%)
Alive	7 (70)	158 (69)
Male gender	8 (80)	122 (53.3)
Race		
African-American	0	16 (7)
Caucasian	8 (80)	122 (53.3)
Asian American	0	27 (11.8)
Latino	2 (20)	21 (9.2)
Other/unknown	0	43 (18.8)
Age at cancer diagnosis, median (IQR)	8.6 (7.5,13.3)	8.4 (4.2,12.5)
Age at cranial radiation therapy, median (IQR)	9.7 (7.9,13.7)	8.7 (4.4,12.8)
Tumor type		
Medulloblastoma	2 (20)	33 (14.4)
High-grade glioma	3 (30)	56 (24.5)
Low-grade glioma	2 (20)	43 (18.8)
Brainstem glioma	0	3 (1.3)
Retinoblastoma	0	19 (8.3)
ALL	0	1 (0.44)
Others	3 (30)	74 (32.3)

ALL: acute lymphoblastic anemia; SD: standard deviation

Table 2

Patient characteristics of those with radiographically detected ICM

Patient	Gender	Cancer Type	Age at Radiation Therapy	Radiation Dose (cGy)	Radiation Field	ICM location	Interval of f/u MRI (year)	Time to ICM detection† (years)	Age at ICM detection (years)
1	male	MB	6	6100	whole brain	left frontal periventricular	1	1	7
2	female	MB	7	6055	posterior fossa	left parietal	1	6	13
3	female	PA	7	5800	posterior fossa	left inferior temporal	1	12	20
4*	male	PA	8	5580	right frontal	right frontoparietal	1	19	28
5*	male	MG	8	5400	left temporal	left temporal lobe	2	13	21
6	male	AA	10	5940	whole brain	bilateral thalami	1	6	16
7	male	BL	11	2400	frontal	frontal subcortical	0	14	26
8	male	MEC	14	5760	parotid	right frontal lobe	1	4	19
9	male	PA	15	5580	whole brain	right periventricular	0	24	39
10*	male	PA	16	6600	right temporal	right temporal parietal	2	11	28

AA = Anaplastic astrocytoma, BL = Burkitt's lymphoma, PA = pilocytic astrocytoma, MB = medulloblastoma, MEC = mucoid epidermal carcinoma, MG = mixed germinoma

* These patients received surgical resection for symptomatic ICM (Patient 4: seizures and headache; Patient 5: headache; Patient 10: L sided numbness, weakness and facial droop)

† presented as years after cranial radiation therapy.